RICE UNIVERSITY

Beamforming on Mobile Devices: A First Study

by

Hang Yu

A THESIS SUBMITTED
IN PARTIAL FULFILLMENT OF THE
REQUIRMENTS FOR THE DEGREE

Master of Science

APPROVED, THESIS COMMITTEE:

Lin Zhong, Chair, Assistant Professor, Electrical and Computer Engineering

Ashutosh Sabharwal, Associate Professor, Electrical and Computer Engineering

Edward Knightly, Professor, Electrical and Computer Engineering

Joseph Cavallaro, Professor, Electrical and Computer Engineering

HOUSTON, TEXAS
APRIL 2011

ABSTRACT

Beamforming on Mobile Devices: A First Study

by

Hang Yu

In this work, we report the first study of beamforming on mobile devices. We first show that beamforming is already feasible on mobile devices in terms of form factor, power efficiency and device mobility. We then investigate the optimal way of using beamforming in terms of power efficiency, by allowing a dynamic number of active antennas. We propose a simple yet effective solution, BeamAdapt, which allows each mobile client in a network to iteratively identify the optimal number of active antennas with fast convergence and close-to-optimal performance. Finally we report a WARP-based prototype of BeamAdapt and experimentally demonstrate its effectiveness in realistic environments. We also complement the prototype-based experiments with Qualnet-based simulation of a large-scale network. Our results show that BeamAdapt with four antennas can reduce the power consumption of mobile clients by more than half compared to omni directional transmission, while maintaining a required network throughput.

Acknowledgements

I would like to firstly thank my advisor, Professor Lin Zhong, who has guided me throughout my academic life at Rice University. He has made significant impact on my way to become a good researcher.

Professor Ashutosh Sabharwal deserves my special thanks for his insightful and inspiring advices to me. This work would never be in current shape without his continuous efforts.

I also appreciate the help from all my other committee members, Professor Edward Knightly and Professor Joseph Cavallaro. Their comments and feedback to this work are of great value.

Finally for all my friends, as well as my parents in China, I am in debt to them. I cannot imagine how I can succeed in my research life without them.

Contents

List of Figures

List of Tables

Chapter 1 **Introduction**

Thanks to the continual decrease of hardware cost, emerging mobile devices are increasingly embracing smart antenna technologies in their wireless interfaces in order to achieve higher data rate and better network connectivity for mobile Internet. For instance, many state-of-the-art mobile devices already employ IEEE 802.11n in their Wi-Fi interfaces, integrating two antennas for supporting a data rate up to 150Mbps. Next-generation Smartphones employing LTE or WiMAX will also implement multiple antennas in their cellular interfaces to support high speed mobile access.

Smart antenna technologies refer to a collection of technologies that employ multiple antennas to transmit and receive radio signals [1]. By properly performing digital signal processing algorithms to the baseband signal, a smart antenna system can significantly improve the link or network performance, e.g., increased capacity or reliability. Broadly speaking, smart antenna technologies include spatial techniques (a.k.a. MIMO) and beamforming, which leverage the multiple antennas in different ways to improve the link or network performance. MIMO intends to utilize the multipath effect to increase either link capacity by spatial multiplexing, or link reliability by diversity. The link performance improvement by MIMO largely depends on the channel condition, i.e., how the sub-channels associated with the antennas are correlated. Beamforming, on the other hand, increases link SNR by properly changing the magnitude and phase of the signals from different antennas so that they are constructively added at the intended receiver. The SNR improvement by beamforming is independent on the channel condition as long as the channel can be accurately estimated.

For a single link, MIMO can increase its capacity by up to *N* where *N* is the number of antennas (number of transmit or receiver antennas, whichever is smaller) [2]; beamforming, however, can only increase the link SNR by up to *N* [1], which according to Shannon theory can be translated into a capacity improvement of approximately *log(N)*. Therefore, in typical mobile environments, with reasonable multipath effect, MIMO is more likely to be beneficial for a single link in terms of capacity improvement. However, MIMO has a much higher antenna spacing requirement than beamforming does, making the implementation of MIMO with a large number of antennas on mobile devices much more challenging.

Equally crucial is the power overhead of both MIMO and beamforming, by their use of multiple active RF chains simultaneously. Our parallel work on MIMO, called RF Chain Management [3], is addressing this power issue by optimizing the tradeoff between link capacity and end device power efficiency. By minimizing the energy per bit for either transmission or reception or both, RF Chain Management can on average increase the device power efficiency by 25% while achieving the required data rate. The optimization, however, is constrained to a single link.

For our work reported in this thesis, we employ beamforming on mobile devices and study its optimal use in terms of power efficiency. Our motivation comes from a key observation towards all current and emerging wireless standards: they assume their mobile accessing clients are omni directional for transmission. As mentioned above, while the multiple antennas on clients can be used as MIMO to improve the rate of each link, we highlight an important fact that current mobile networks are greatly limited by interference instead of individual link capacity, as the number of mobile devices

explodes. As a result, compared to MIMO which attempts to improve link rate, beamforming is preferably appreciated by current mobile networks to combat with the interference problem.

While beamforming has been well studied and already deployed for base stations, access points, and vehicles, it has never been examined for mobile devices due to three physical challenges of mobile devices: small size, mobility, and limited power. Naturally, the first question one may ask is: *is beamforming feasible for mobile devices?* We answer this question by examining the three challenges. (*i*) First, we show that single-user beamforming with two to four antennas can fit into reasonably sized mobile devices with a linear or circular array. (*ii*) Second, we experimentally demonstrate that the beamforming gain remains high even when the device can not only move but also rotate. (*iii*) Finally, using data from research prototypes and emerging products, we show that beamforming can be even more power-efficient than its single antenna counterpart, by making an increasingly profitable tradeoff between transmit and circuit power. More importantly, we reveal the existence of the optimal number of active antennas, or the optimal *beamforming size*, which minimizes the device overall power. We show that the optimal beamforming size is dependent on channel condition and required link capacity, which strongly suggests an adaptive use of beamforming that adjusts the beamforming size and turns off idle antennas for power efficiency.

Such adaptive beamforming is straightforward to realize for a single link because the optimal beamforming size can be analytically calculated. However, with multiple interfering clients, identifying the optimal beamforming size for each client is very challenging, due to not only the absence of an analytical solution, but also the

requirement of client collaboration to enumerate all beamforming size combinations. Therefore, the second question we seek to answer is: *can each client in a large-scale network individually identify its beamforming size that collectively approaches the optimal tradeoff with minimum network power consumption?* We answer this question by proposing BeamAdapt, a distributed solution with which each client optimizes its beamforming size *without* coordination with others. The key idea of BeamAdapt is simple: each client iteratively adjusts its beamforming size solely based on the SINR at its own receiver. We show that BeamAdapt has guaranteed convergence and closely approaches the optimal.

We evaluate BeamAdapt first through a prototype-based experiment of a two-link network and then a Qualnet-based simulation of a large-scale network. Our experimental results show that BeamAdapt consumes only 5% higher power compared to a genie-aided solution as the performance bound of BeamAdapt in reality. For our Qualnet-based simulation, we realize BeamAdapt in the context of modern cellular networks. We show that by cleverly leveraging uplink power control, BeamAdapt can be easily realized on mobile clients with trivial protocol modification. We show that within a large-scale cellular network, BeamAdapt with four antennas can reduce power consumption of the client wireless transceiver by 54% with similar network throughput.

In summary, we make the following technical contributions toward beamforming on mobile devices:

- We report the first feasibility study of beamforming on mobile devices in terms of form factor, power efficiency, and device mobility.

- We provide a simple yet effective solution, BeamAdapt that allows each client in the network to rapidly identify the optimal beamforming size to achieve required capacity with near-optimal power efficiency. The simplicity of BeamAdapt is indeed a strength, allowing its immediate realization on cellular mobile devices.
- We report a prototype of BeamAdapt based on the WARP platform and a system design for realizing BeamAdapt in cellular networks.

We note that BeamAdapt can be extended in three important ways. Firstly, while we propose BeamAdapt for transmit beamforming in this work, receive beamforming on mobile clients can similarly adopt BeamAdapt for power efficiency, with an even simpler formulation. Secondly, BeamAdapt is general for any receiver architectures. That assumed in this work, i.e., treating interference as noise, is in fact an effective architecture to leverage the benefit of BeamAdapt. Finally, BeamAdapt leverages the beamforming gain to achieve client power efficiency given the capacity requirement. The beamforming gain can be reciprocally used to improve the capacity given the client power constraint, indicating a dual formulation of BeamAdapt.

The rest of the paper is organized as follows. Chapter 2 presents background knowledge on beamforming. Chapter 3 presents a feasibility study of using beamforming on mobile devices. Chapter 4 provides the theoretical framework of BeamAdapt. Chapter 5 provides the prototype-based evaluation of BeamAdapt and Chapter 6 offers its simulation-based counterpart. Chapter 7 addresses related works and Chapter 8 concludes the paper.

Chapter 2 **Beamforming Primer**

Unlike omni directional transmission with a single antenna, beamforming uses a group of antennas to increase the SNR of the received signal. Each antenna includes a passive antenna and a devoted RF chain that bridges the baseband and RF signal. Beamforming operates by assigning different weights to the baseband signal and then transmitting them through multiple antennas, or

$$\boldsymbol{x}(t) = \boldsymbol{w} \cdot s(t), \boldsymbol{x}(t) = \big(x_1(t), \cdots, x_N(t)\big), \boldsymbol{w} = (w_1, \cdots, w_N),$$

where the baseband signal, weight vector and output signal vector are denoted as $s(t)$, $\boldsymbol{w}$ and $\boldsymbol{x}(t)$, respectively. The beamforming gain G is defined as the ratio of the received SNR with beamforming to that with a single antenna. Noticeably, G is dependent on the number of active antennas, or *beamforming size*, N.

2.1 Antenna Spacing

Antenna spacing also has a significant impact on the beamforming gain. When the antenna spacing is sufficient, the maximal beamforming gain, G_{max}, is equal to the beamforming size N [2], or $10\log(N)$ in dB. It is achieved when signals from each transmit antenna add coherently at the receiver, independent on the direction of the receiver or the angle of the antenna array relative to the receiver.

When the antenna spacing decreases, the beamforming pattern becomes wider as shown by Figure 1 (Left), because the angular resolution does not suffice to suppress the correlation between individual signals. As shown by Figure 1 (Right), when the antenna spacing drops below certain threshold, the peak beamforming gain will drop due to the

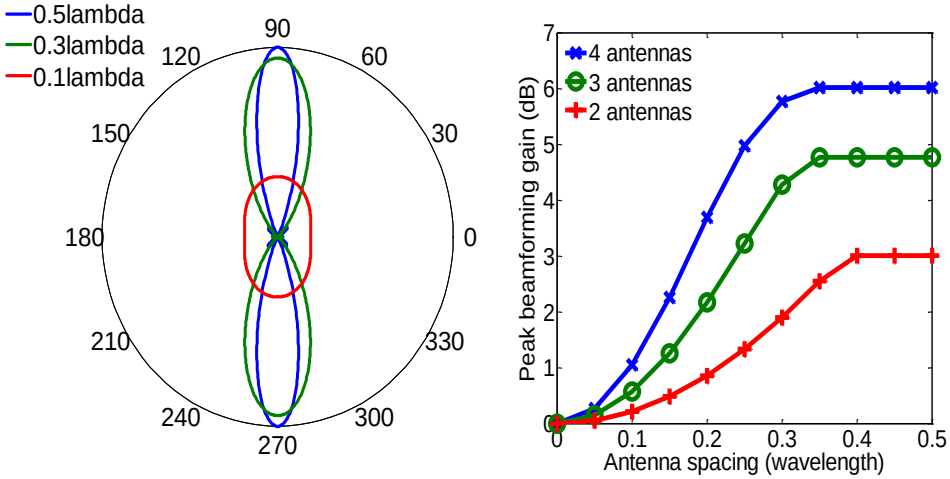

Figure 1: (Left) Beamforming pattern of a linear array with four antennas, under different antenna spacing; (Right) Beamforming gain with different antenna spacing, for beamforming size from two to four.

power leakage toward a wider range of directions. The minimum requirement for maintaining the maximal beamforming gain depends on the number of antennas and is typically 0.3-0.4λ where λ is the wavelength of the carrier signal.

In this work we only consider *single-user beamforming*, where the transmitter optimizes its weight vector for a single receiver [2]. We note that other multi-antenna techniques typically have more demanding requirement for antenna spacing. *Multi-user beamforming* [3] and *null beamforming* require the antenna spacing be above 0.5λ [4], in order to exploit additional degrees of freedom when choosing the weight vector. *Spatial multiplexing/diversity techniques*, a.k.a. MIMO techniques, typically need an antenna spacing of multiple wavelengths to operate with a satisfactory capacity improvement [4]. Apparently, they do not fit into iPhone-like mobile devices for the frequency bands in use today (2 to 5GHz).

2.2 Channel Estimation

To guarantee that the signals from multiple transmit antennas add coherently at the receiver, beamforming requires channel knowledge at the transmitter. In single-user beamforming, the weight vector is assigned as $\boldsymbol{w}=\boldsymbol{h}^*$, where $\boldsymbol{h}$ is the channel vector with each of its elements representing the channel coefficient between a transmit antenna and the receiver. The channel vector $\boldsymbol{h}$ is often denoted as *channel state information* (CSI). For transmit beamforming, CSI can be obtained through either closed-loop or open-loop estimation. For closed-loop estimation, the receiver leverages the training symbols sent from the transmitter to calculate the channel coefficients and sends it back to the transmitter. For open-loop CSI estimation, the transmitter estimates the reverse channel when receiving and uses it for transmitting. Apparently, open-loop CSI estimation requires channel reciprocity to be effective.

2.3 Power Characteristic

For single-user beamforming, given $\boldsymbol{h}$, the weight vector $\boldsymbol{w}$ is also given without the need of any additional computation. This is different to MIMO techniques which often need considerable signal encoding and processing even at the transmitter. As a result, single-user beamforming incurs little power overhead by baseband processing and we next focus on its RF power characteristic. Figure 2 illustrates the major RF hardware components of a beamforming transmitter. The transmitter consists of multiple RF chains, each of which is connected to an antenna. When we say an antenna is active, we mean that the RF chain connected to the antenna is powered on and active. When a

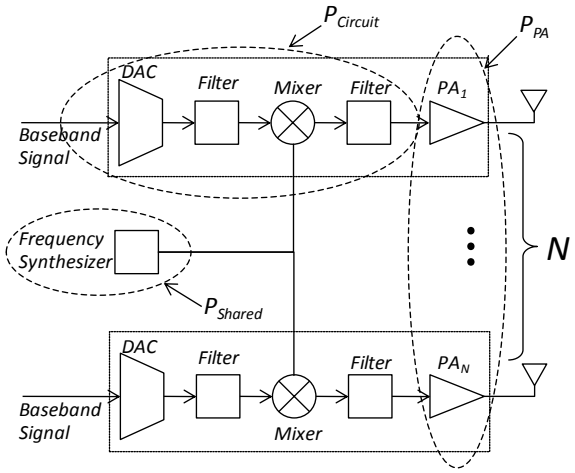

Figure 2: RF components of a beamforming transmitter.

beamforming antenna is not in use, the corresponding RF chain can be powered off to conserve power.

As shown by Figure 2, the transmitter power consumption can be decomposed into that of the circuitry shared by all active RF chains, i.e. the *frequency synthesizer*, denoted as P_{Shared}, and that of each active RF chain. The power contributed by each active RF chain can be further broken down to that by the *power amplifier*, and that by the rest of the chain, denoted as $P_{Circuit}$. Since we assume identical power amplifiers for all RF chains, we combine their power consumption, jointly denoted as P_{PA}, with the output power from transmit antenna included. Clearly, P_{PA} is dependent on the total transmit power, P_{TX}, while $P_{Circuit}$ is constant irrespective of P_{TX}.

We model P_{PA} as $P_{PA}=P_{TX}/\eta$, where η is the efficiency of the power amplifier. The efficiency η is usually dynamic depending on the transmit power, and here we approximate η as a linear function of P_{TX} [5] while the power amplifier itself is not linear. As a result, the total power P can be fairly accurately modeled as

$$P = \frac{P_{TX}}{\eta(P_{TX})} + NP_{Circuit} + P_{Shared} \quad (1)$$

In the rest of the paper, we adopt parameters as follows: η_{min}=0.3, η_{max}=0.5, $P_{Circuit}$=48.2mW, P_{Shared}=50mW. They are chosen partially based on [5, 6] as well as all recent CMOS wireless transceiver designs we have collected (see Section 3.3). Those parameters are on par with state-of-the-art transceiver designs in 2-5GHz band [7].

Chapter 3 **Feasibility Study**

The first reaction one may have toward beamforming on mobile device is likely to be: *is it feasible at all* (possibly thinking of the bulky, power-hungry Phocus Array system [8])? In this section, we examine the three key physical challenges to put beamforming on mobile devices: size, mobility, and power efficiency. Our key conclusion after a careful examination is: beamforming not only is feasible for reasonably sized mobile devices but also can improve their power efficiency if used properly.

3.1 Form Factor

With the advancement of semiconductor technologies, multiple RF chains are already being integrated into a single transceiver chip, e.g., [9]. Therefore, the form factor challenge posed by beamforming only stems from its antenna spacing requirement. As discussed in Section 2.1, beamforming typically requires the antenna spacing to be higher than 0.3λ-0.4λ or 4.5cm-6cm in the 2GHz band.

There is no obstacle for medium-size mobile devices such as Tablets and NetBooks to embrace a beamforming array with fours antennas, in either a linear or a circular array. Even small-size mobile devices such as iPhone-like Smartphones can accommodate two antennas in a linear array or four in a circular array. Even if the antenna spacing requirement cannot be strictly satisfied, the corresponding drop of the beamforming gain will be approximately linear according to Figure 1, and one can still achieve a significant gain compared to a single antenna.

It is also worth noting that multi-antenna solutions using passive directional antennas reported in [1] do not have much antenna spacing requirement because only one directional antenna is active at a time. However, the solution requires all the directional antennas to be properly oriented, which imposes a different and even larger form factor challenge.

3.2 Mobility

A mobile device can not only move but also rotate. Recent work has shown that beamforming with predefined beam patterns can cope with vehicular mobility very well, e.g., [10, 11]. However, real-time beamforming poses a new challenge due to the requirement of accurate CSI, including only not the magnitude but also the phase of the channel coefficients which are largely affected by device rotation. Therefore, next we focus on evaluating the beamforming gain under device rotation since device rotation can potentially introduce faster channel variation than mobility can.

We perform the experiments using the WARP software radios [12]. We build a circular array with four antennas on one WARP board as the mobile client, and use a single antenna at the other WARP board as the infrastructure node. The client and infrastructure nodes are placed close to the allowed range with a moderate SNR (5dB), i.e. 10 meters in our experiments. The client node continuously sends training symbols to the infrastructure node every 10ms and the latter sends back the estimated CSI through an Ethernet cable. Therefore, the mobile client updates the CSI each 10ms, calculates the weight vector and forms a beam. To challenge the CSI estimation, we rotate the client node with a computerized motor at 90 °/s and 180 °/s respectively, while realistic mobile

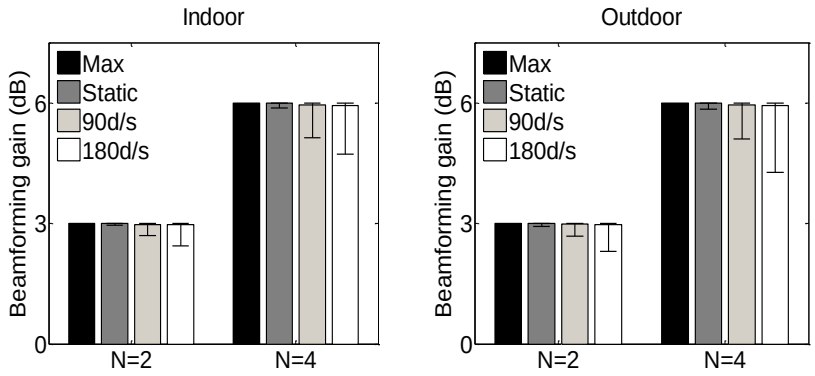

(a) CSI estimation per 10ms

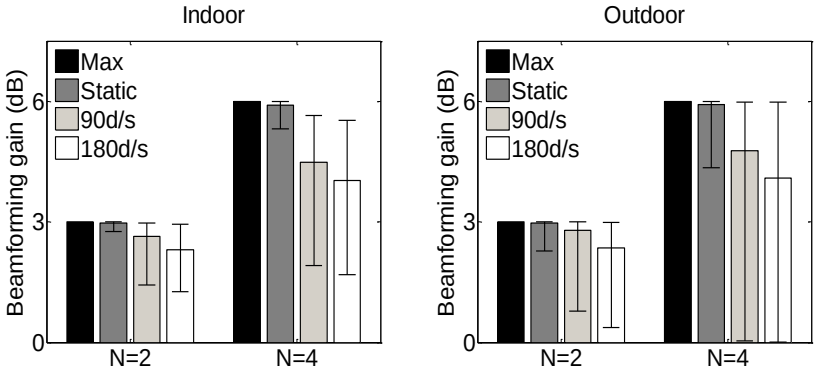

(b) CSI estimation per 100ms

Figure 3: Beamforming gain under CSI estimation with various client rotation speeds. We show the results in different environments as well as with different CSI estimation frequencies.

devices rotate at a much slower speed, e.g. 10 °/s as the median and 120 °/s as the upper bound [1]. We repeat the experiments both indoor and outdoor. While we could not simultaneously examine different beamforming sizes and different CSI estimation frequencies in real time, we have collected traces of the channel coefficients and emulate the channel offline. That is, we replay the channel using the recorded traces but assume different beamforming sizes (2 and 4), and different CSI estimation frequencies (10ms

and 100ms). Since the beamforming gain is only dependent on the CSI, the offline emulation gives identical results as real-time evaluation does.

The key question we aim to answer is: *what is the impact of device rotation on CSI estimation and corresponding beamforming gain?* To see this, Figure 3 shows the average beamforming gain under CSI estimation with different rotation speeds of the client. In each sub-figure of Figure 3, four values of beamforming gain for each beamforming size are shown: the upper bound given by perfect CSI (Max), the one given by estimated CSI with stationary client (Static), the one given by estimated CSI with rotating client at 90 °/s (90d/s), and the one given by estimated CSI with rotating client at 180 °/s (180d/s).

When the CSI estimation interval is 10ms, the CSI can be very accurate even with client rotational speed of 180 °/s. As a result, the maximal beamforming gain, i.e. 3dB and 6dB with N=2 and N=4 respectively, can be achieved. When the interval is increased to 100ms, the beamforming gain will be affected by client rotation. The rotation has higher impact for larger beamforming sizes due to a more focused beamforming pattern. Therefore, we conclude that even under high speed device rotation such as 180 °/s, beamforming can still be effective with reasonable CSI estimation intervals, e.g., 10ms. In contrast, the solution in [1] achieves a much lower gain relative to the maximal allowed by the passive directional, e.g. 3dB using 5dBi and 8dBi antennas. Finally, we observe that the performance of CSI estimation is more stable indoor, due to richer multipath effect to compensate bad directions. This can be seen from the range of the beamforming gain in each sub-figure.

3.3 Power Efficiency

Although single-user beamforming incurs negligible power overhead in baseband processing, it increases the power of RF circuitry by simultaneously using multiple active RF chains compared to a single antenna. While RF integrated circuits improve slower than their digital counterparts, their power efficiency still improves significantly over years. To illustrate this trend, we have examined the CMOS wireless transceiver realizations reported in ISSCC [13] and JSSC [14], the top conference and journal for semiconductor circuits, from 2003 to 2010, and show their circuit power consumption, $P_{Circuit}+P_{Shared}$, in Figure 4 (Left). The figure clearly shows the continuous improvement in the power efficiency of both SISO and MIMO transceivers. As semiconductor process technologies continue to improve, $P_{Circuit}$ and P_{Shared} will continue decreasing. As a result, P_{PA} will increasingly dominate the total power consumption.

By focusing the transmit power toward the intended direction, beamforming can reduce P_{TX} and P_{PA} and therefore even improve the power efficiency. Clearly, beamforming makes a tradeoff between transmit and circuit power: with a beamforming size of N, the transmit power can be reduced to $1/N$ compared to a single antenna due to the beamforming gain. Note that beamforming is able to yield a total transmit power reduction instead of that of each antenna, i.e. the reduction is not because of the allocation of transmit power into multiple antennas.

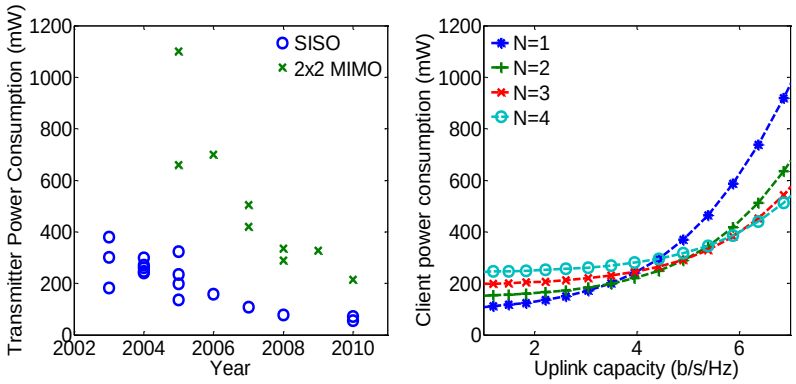

Figure 4: (Left) Transmitter power trend from designs in ISSCC and JSSC; (Right) Client power consumption to deliver a range of link capacity.

Table 1: Simulation settings for the power tradeoff analysis.

Parameters	Values
Distance	**0.5km**
Max beamforming size	**4**
Power decay factor	**4**
Receiver noise	**-170dBm/Hz**
Channel bandwidth	**5MHz**
Carrier frequency	**2GHz**

We next briefly analyze this tradeoff between transmit and circuit power. For simplicity, we consider a single uplink channel from a mobile client to its infrastructure node and assume line-of-sight (LOS) propagation and the settings specified in Table 1. Figure 4 (Right) shows the client power consumption calculated by Equation (1) to deliver a range of link capacity for beamforming sizes from one to four. One can make two important conclusions from the figure. (*i*) First, beamforming (N>1) is already more efficient than omni directional transmission (N=1) when delivering a capacity of

3.2b/s/Hz or higher. (*ii*) Second, the larger the required link capacity, the larger the most power efficient beamforming size. This shows that beamforming is increasingly desirable in delivering higher capacity.

Chapter 4 **Adaptive Beamforming on Mobile Devices**

The above findings above suggest an adaptive beamforming system that adjusts the beamforming size for the optimal tradeoff between transmit and circuit power, according to link capacity requirement. Next we show that to achieve the best tradeoff in a network is indeed non-trivial and, therefore, provide a simple yet effective solution, BeamAdapt.

4.1 Key Tradeoff and Challenge

As shown above, the optimal beamforming size varies according to the required link capacity. Given the transmit power decay factor and distance, one can derive the required transmit power for omni directional transmission, P_O, to achieve certain link capacity. Using Equation (1), we can calculate the optimal beamforming size as

$$N_{opt} = \sqrt{P_O/C_1 P_{Circuit}} - C_2 P_O/C_1 \quad (2)$$

where C_1 and C_2 are constants determined by the power amplifier. Again, beamforming with more antennas is increasingly more efficient as $P_{Circuit}$ decreases according to the continual progress in semiconductor technologies.

While the optimal tradeoff given by N_{opt} appears straightforward to identify with a single link (P_O is uniquely decided by the required capacity or SNR), it is challenging to determine in a network with multiple links. This is because P_O is determined by SINR instead of SNR due to interference. Meanwhile, different beamforming sizes will generate different interference toward other receivers, implicitly impacting their own SINR. As a result, the optimal beamforming size can no longer be calculated by Equation (2).

Nonetheless, the tradeoff between transmit and circuit power is still valid and there exists a most power efficient beamforming size for each client that collectively minimizes the aggregated client power consumption, or *network power consumption*. The immediate question we seek to answer is: *how could clients of a large network identify their most power-efficient beamforming sizes that collectively lead to the minimum network power consumption?*

4.2 Problem Formulation

Since we are interested in client power efficiency, we seek to minimize $P_{Network}$, the aggregated power consumption by all clients in a network, with a constraint that the capacity, or equivalently the SINR of each link i, $SINR_i$, must be equal to certain target value, ρ_i. The reason of separately constraining individual links is that different links usually have different capacity requirements. In addition, the beamforming size N_i must be integers no greater than $N_{i,max}$, where $N_{i,max}$ is the maximum number of antennas on client i.

Therefore, we formulate the optimization problem as:

$$\text{minimize } P_{Network} = \sum_{i=1}^{M} P_i\,(P_{TX,i}, N_i)$$

$$\text{s.t. } SINR_i(\boldsymbol{P}_{TX}, \boldsymbol{N}) = \rho_i, 1 \le N_i \le N_{i,max}$$

where P_i is the power consumption of client i and

$$\boldsymbol{P}_{TX} = \left(P_{TX,1}, \cdots, P_{TX,M}\right), \boldsymbol{N} = (N_1, \cdots, N_M).$$

Solving the above optimization problem is very challenging. Firstly, each of the SINR constraints is a function of all $2M$ optimization variables. The SINR function is non-convex with respect to these variables, yielding the non-convexity of the problem.

Secondly, there is no closed-form formulation of the beamforming gain G to unintended receivers as a function of N. Its dependence on the receiver direction makes low-order approximation hardly possible. Finally, the integer constraint on N_i renders a NP-hard mixed integer programming (MIP) problem [15]. While an exhaustive search algorithm can ultimately offer the solution, the complexity can be as high as $O\left(\prod_{i=1}^{M}(N_{i,max})\right)$, which becomes prohibitively complex as M grows. Most importantly, such a brute-force algorithm requires all the clients have knowledge of each others' actions in order to enumerate all beamforming size combinations, and cooperatively choose their beamforming sizes.

To tackle this problem, we introduce BeamAdapt, a simple yet effective algorithm that works in a distributed manner: each client simply performs individual optimization on the beamforming size without cooperation.

4.3 Distributed Algorithm: BeamAdapt

First we decompose the problem into multiple, individual sub-problems, i.e., the ith link's problem (i=1,2,$\cdots M$) is

$$\min P_i \quad \text{s.t. } SINR_i = \rho_i.$$

The optimal ($P_{TX,i}$, N_i) is determined iteratively. Let us temporally omit the subscript i below since all clients employ the same algorithm. We assume the transmit power and beamforming size are $P_{TX}^{(k-1)}$and $N^{(k-1)}$ for the (k-1)th iteration, and the received SINR is $SINR^{(k-1)}$, then for the kth iteration, $P_{TX}^{(k)}$ and $N^{(k-1)}$ are updated by solving the following optimization problem:

Algorithm 1: Identify the optimal beamforming size and transmit power for each client by BeamAdapt

Input: SINR requirement ρ, max beamforming size N_{max}

Output: optimal beamforming size N^{opt}, transmit power P_{TX}^{opt}

$\left(P_{TX}^{(0)}, N^{(0)}\right) = (P_{TX}^{(0)}, 1)$,$SINR = 0$,$P_{min} = +\infty$
$\left(P_{TX}^{opt}, N^{opt}\right) = \left(P_{TX}^{(0)}, N^{(0)}\right)$
while $|SINR - \rho| \geq \varepsilon$
    for $N^{(k)} \leq N^{(k+1)} \leq N_{max}$
        Compute $P_{TX}^{(k+1)}$,$SINR$
        $P = P_{TX}^{(k+1)}/\eta + N^{(k+1)}P_{Circuit} + P_{Shared}$
        if $P \leq P_{min}$
            $\left(P_{TX}^{opt}, N^{opt}\right) = \left(P_{TX}^{(k+1)}, N^{(k+1)}\right)$
            $P_{min} = P$
        end
    end
end
return $\left(P_{TX}^{opt}, N^{opt}\right)$

$$\min_{P_{TX}^{(k)}, N^{(k)}} P_{TX}^{(k)}/\eta + N^{(k)}P_{Circuit} + P_{Shared}$$

$$\text{s.t. } \frac{P_{TX}^{(k)}N^{(k)}}{P_{TX}^{(k-1)}N^{(k-1)}} = \frac{\rho}{SINR^{(k-1)}},\ N^{(k)} \geq N^{(k-1)}.$$

The initial beamforming size is set to one, i.e. $N^{(0)} = 1$, while $P_{TX}^{(0)}$ can be arbitrary.

The iteration stops when $\left|SINR^{(k)} - \rho\right| \leq \varepsilon$, where ε can be set according to an accuracy requirement. In each iteration, $(P_{TX}^{(k)}, N^{(k)})$ can be obtained by searching among feasible beamforming sizes, with a complexity of $O\left(\max(N_{i,max})\right)$. Algorithm 1 shows the pseudo-code of the algorithm. We note that when *M*=1, the problem reduces to single-link optimization offering the same solution as Equation (2).

4.4 Convergence of BeamAdapt

The iteration process of BeamAdapt is guaranteed to converge. Next we provide a brief yet sufficiently illustrative proof. The two key facts we leverage are: (*i*) whenever the beamforming sizes are fixed, the iteration of BeamAdapt is isomorphic to a distributed power control algorithm [16] that ensures convergence; and (*ii*) the change of the beamforming size *N* of each client is monotonous. That is, the beamforming size can only increase during iteration.

Therefore, we divide the iteration process into multiple stages, $k_l (1 \leq l \leq L)$, where during each stage *N* is constant and only P_{TX} changes. The current stage k_l evolves into k_{l+1} when *N* changes for any one link. Based on the monotonicity of *N* we have the following inequality

$$L \leq \prod_{i=1}^{M} (N_{i,max}) < +\infty,$$

which indicates a finite number (*L*) of stages.

During each stage, the beamforming size is fixed; therefore the original problem turns in to

$$\min\ P_{Network} = \sum P_i(P_{TX,i}), \text{ s.t. } SINR_i(\boldsymbol{P}_{TX}) = \rho_i.$$

This problem is isomorphic to the power control problem where a distributed algorithm ensures convergence [16]. As a result, during each stage (k_l) the power control component either converges, or it moves onto a new stage. Since the number of potential stages *L* is finite, the overall algorithm is guaranteed to converge.

4.5 Performance Bound of BeamAdapt

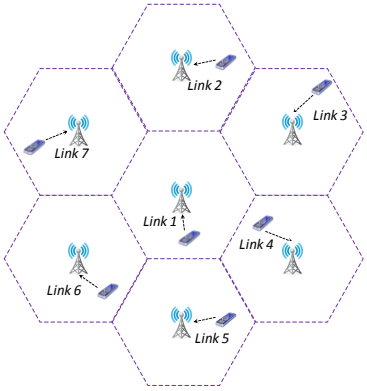

(a) Network configuration

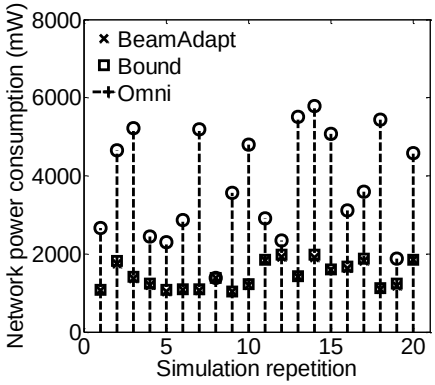

(b) Network power comparison

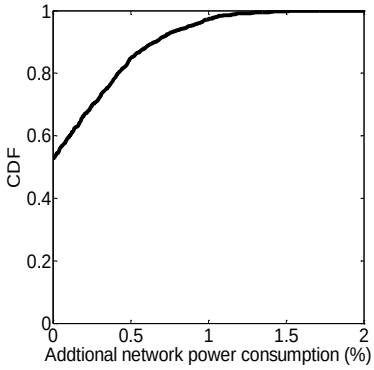

(c) CDF of the additional power consumption by BeamAdapt

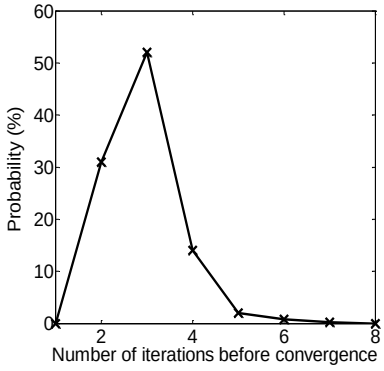

(d) PDF of the convergence speed of BeamAdapt

Figure 5: Empirical results for the performance bound and convergence speed of BeamAdapt.

We next investigate how fast BeamAdapt converges and how good its steady-state performance is. It is possible that BeamAdapt converges to a sub-optimal solution. Unfortunately, the performance bound of BeamAdapt is not analytically obtainable, again due to the non-convexity of the optimization problem and the integer constraints on the beamforming size. Therefore, we have to rely on empirical methods to study the performance bound. We employ a seven-cell network as a first-order approximation of a

large-scale infrastructure network as shown in Figure 5 (a): we assume seven infrastructure nodes are evenly distributed in the space. Other settings are similarly adopted from

Table 1. To eliminate the dependency of BeamAdapt on the client location, we repeat the simulation extensively with random locations of the clients. Therefore, we are in fact averaging the performance of BeamAdapt with various network configurations.

Figure 5 (b) shows a few samples of the network power consumption of BeamAdapt, and its upper bound given by the theoretically optimal solution using a brute-force algorithm with client cooperation. The figure also shows the performance of omni for comparison. Clearly, the performance of BeamAdapt is very close to the optimal and much better than that of omni. Figure 5 (c) shows the CDF of the additional network power consumption by BeamAdapt compared to its bound: BeamAdapt indeed converges to the optimal solution with a probability of 55%, and only incurs 0.5% additional power compared to the optimal solution when it converges to a sub-optimal.

Using the same network configuration, we can also evaluate the convergence speed of BeamAdapt, with Figure 5 (d) showing the PDF of the number of iterations to achieve a small ε, i.e., 0.1% in our simulation. Clearly, BeamAdapt often converges rapidly, i.e. with typically less than three iterations to get a stable SINR.

Chapter 5 **Prototype-based Evaluation**

In Chapter 3.2 we experimentally showed the feasibility of beamforming on mobile devices with a close-to-maximum beamforming gain even when the mobile client rotates at 180 °/s. However, compared to static beamforming with a fixed number of active antennas, BeamAdapt faces a new challenge due to its iterative nature: *are mobile clients with BeamAdapt able to timely identify the right number of antennas and transmit power in real-time so that the required SINR is achieved with maximal power reduction?* To answer the question, we use WARP to experimentally evaluate the feasibility of BeamAdapt in realistic environments.

We must note that BeamAdapt is a general technique compatible with any infrastructure network architecture such as WLAN or cellular. Since we are not able to conduct experiments on cellular bands due to the lack of license, we use ISM band (2.4GHz) to validate the feasibility of BeamAdapt. Our Qualnet-based evaluation in Section 6, however, will complementarily show the power saving and network throughput performance of BeamAdapt within a large-scale cellular network.

5.1 BeamAdapt Prototype

We realize BeamAdapt using WARPLab, a framework that facilitates rapid prototyping of physical layer designs and algorithms. WARPLab allows symbol-level access to the wireless transceivers embedded on the WARP board, which we leverage to realize the key functionalities of BeamAdapt including beamforming, transmit power and beamforming size adaptation, and SINR measurement. In WARPLab, all WARP nodes

are connected through an Ethernet router and a laptop with MATLAB interface is used to control the nodes, implement the algorithm and collect the data.

We have built two types of WARP nodes: one with four antennas implementing BeamAdapt as the mobile client node and the other with a single antenna as the infrastructure node. Since we assume the simplest receiver architecture for BeamAdapt, i.e. treating interference as noise, the performance of BeamAdapt is independent on the number of antennas on the infrastructure node. The physical wireless channel is assumed as the uplink channel from client node to infrastructure node, while an Ethernet cable is used to emulate the downlink channel. Since we are only interested in client transmission (uplink channel), we generate dummy frames only at the client node and continuously send them to the infrastructure node.

5.2 Experiment Setup

We test the prototype under two physical environments: one inside an office building and the other on an empty lawn, both in a university campus. The former represents a typical indoor environment while the latter outdoor. We use four WARP nodes, including two client nodes and two infrastructure nodes, to form a two-link network. Figure 6 shows our setup using WARPLab and Figure 7 shows the locations of the client and infrastructure nodes.

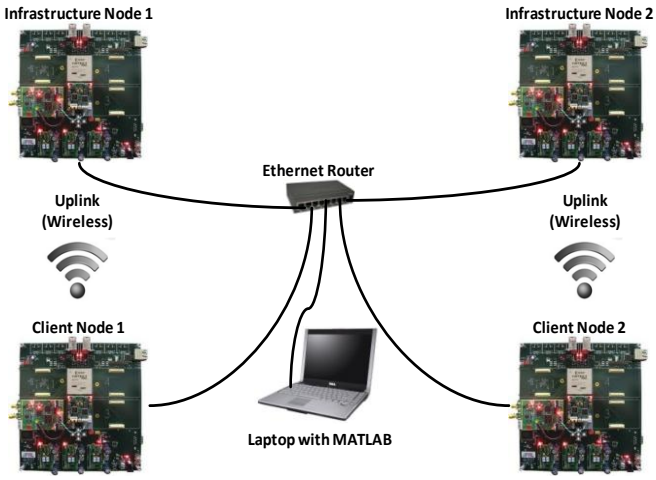

Figure 6: WARPLab setup for the evaluation of BeamAdapt.

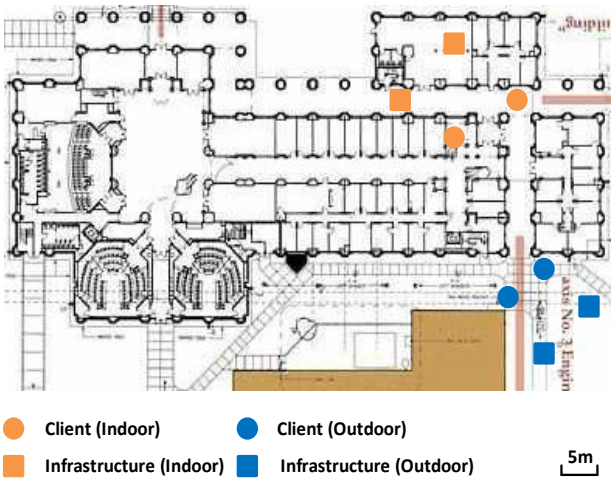

Figure 7: Environment layout for the evaluation of BeamAdapt.

While in realistic wireless networks there might be more links that interfere with each other, we consider this two-link network as a reasonable setup for experiments. Firstly, the two-link network is a widely used model in wireless network researches [4], due to its simplicity and generality. Secondly, even though in realistic such as cellular networks there are more than two base stations within the coverage of a mobile client, the client is often mainly interfering with only one additional base station, due to the distributed

fashion of placing base stations in a certain area and that each client often connects to the closest base station. Finally, since we have selected the ISM bands and the environments of our experiments have continuous but unpredictable wireless transmissions, there are indeed other interference sources at the infrastructure nodes.

In our experiments, we add both movement and rotation to the two client nodes, by manually moving and rotating them. The rotation speed is from zero to one hundred twenty degrees per second, consistent with [1]. The movement is about zero to one meter per second. Due to the limitation of WARPLab that the WARP boards have to be connected by Ethernet cables, we can only add pedestrian movement speed in the experiment but will simulate a much higher speed in the Qualnet simulation in Chapter 6.

5.3 Experimental Findings

We examine the effectiveness of BeamAdapt in realistic environments with two key metrics, received SINR at the infrastructure node and power consumption by the client node. Apparently, they jointly represent the key functionality of BeamAdapt according to our formulation in Section Chapter 4. For received SINR, we examine whether BeamAdapt can closely approach the required SINR even with iteration and client mobility. For power consumption, we compare the power consumption of BeamAdapt with a genie-aided solution which can always correctly pick the right beamforming size and transmit power without the need of iteration. Clearly, the genie-aided solution can achieve maximal power reduction. To realize the comparison, we recorded traces the channel coefficients during all our measurements and replayed the channel offline to emulate the genie-aided solution.

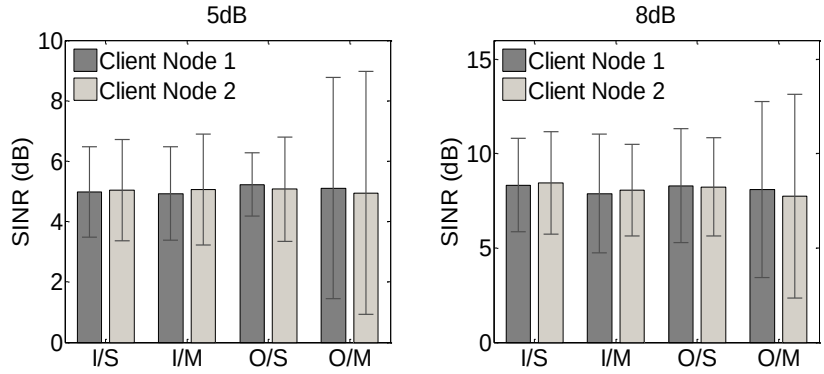

Figure 8: Received SINR at the infrastructure node in the experiments.

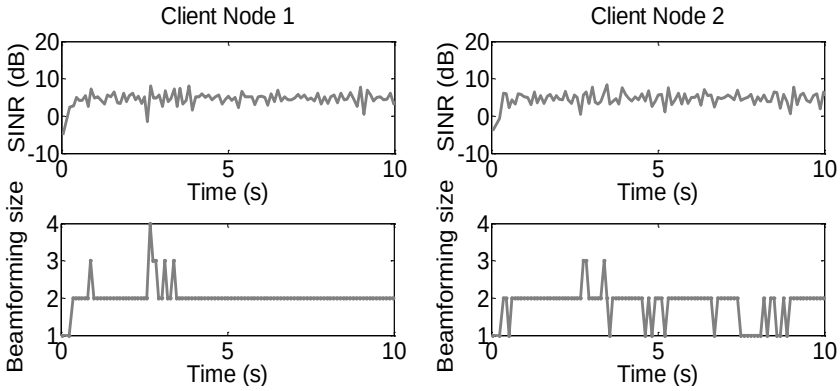

Figure 9: Received SINR and beamforming size at a glance.

5.3.1 Received SINR

We first report the received SINR at the infrastructure nodes. To maximally leverage the range of WARP nodes without losing generality, we assume moderate SINR, e.g. 5dB and 8dB as the constraint. Figure 8 shows the mean and variance of the received SINR at the two infrastructure nodes, for four scenarios: Indoor/Static (I/S), Indoor/Mobile (I/M), Outdoor/Static (O/S), and Outdoor/Mobile (O/M).

We report two key findings from the figure. (*i*) First, on average BeamAdapt can closely approach the required SINR, i.e. 5dB and 8dB respectively, for both stationary and mobile client nodes. In most of the scenarios the standard variance is below 3dB,

meaning that the BeamAdapt iteration does not render significant SINR deviation from the target value. (*ii*) Second, in the outdoor/mobile scenario BeamAdapt yields much higher variance of the received SINR. This is consistent to our observation of the beamforming gain in Section 3.2, due to the lack of compensation by multi-path effect to the out-of-dated channel and beamforming size.

Figure 9 shows a ten-second snapshot of the received SINR as well as the beamforming size of two infrastructure nodes. Clearly, most of the time BeamAdapt is able to timely cope with channel variation and achieves a stable SINR, while the beamforming size is indeed being adapted. We have chosen the Indoor/Mobile scenario to show in the figure while the other scenarios exhibit similar characteristics, as demonstrated by Figure 8

While BeamAdapt on average achieves the required SINR, it does not guarantee that the SINR is above the target value. This is due to the formulation of BeamAdapt that seeks to use the exact amount of power to achieve certain capacity. Nonetheless, BeamAdapt will not lead to a large outage probability, since one can simply leave a SINR margin and set the required SINR in BeamAdapt a bit higher than the actual intended value. For example, if a SINR of 5dB is needed, one can set 8dB as the constraint in BeamAdapt and it will maintain the SINR above the threshold with a probability of 87% according to our results.

5.3.2 Power Consumption

We next compare the power consumption of BeamAdapt with that of the genie-aided solution. It is important to highlight that given the transmit power and beamforming size,

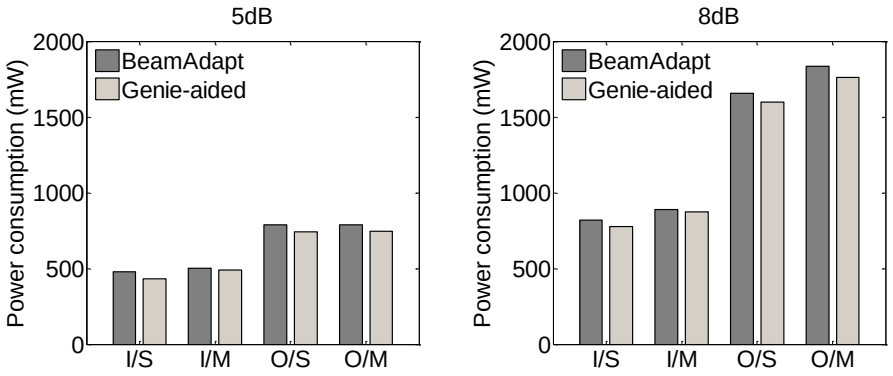

Figure 10: Power consumption of the client nodes for BeamAdapt and genie-aided solution in the experiments.

the power consumption is calculated using the power model in Section 2.3 instead of measurements. This is because the WARP node uses FPGA board and programmable RF board to enable customization, and therefore its power consumption is not optimized and not comparable with realistic beamforming transceivers. Therefore, we use the authentic transmit power but emulate the circuit power to achieve a rational estimation.

Figure 10 shows the average power consumption of BeamAdapt and the genie-aided solution. Clearly, in all scenarios BeamAdapt closely approaches the theoretically minimum power consumption given by the genie-aided solution, yielding only 5% higher power on average. We note that the genie-aided solution has removed all the imperfections of BeamAdapt in reality, such as converging to a sub-optimal solution, procedure of iteration, and drop of beamforming gain due to mobility. Therefore, it is the strict upper bound of the power saving performance of BeamAdapt. Not surprisingly, the additional power consumption in our experiments is larger compared to that in Figure 5 (c), due to the consideration of all realistic imperfections of BeamAdapt listed above.

Chapter 6 Evaluation of BeamAdapt in Cellular Networks

To complement the prototype-based evaluation, we next use simulation to evaluate BeamAdapt with a large-scale network. To achieve a close-to-reality evaluation, we adopt current cellular protocols and introduce a system design of BeamAdapt that is realizable with trivial protocol modification. We employ the simulation tool Qualnet [17] for its open-source feature and support of cellular protocols.

6.1 Cellular-based System Design

We realize BeamAdapt in the mobile accessing clients in a cellular network and again focus on uplink transmission. Due to its distributed property, BeamAdapt relieves clients in the network from inter-client cooperation thereby entails minor protocol modification. There are two key concerns regarding the system realization of BeamAdapt. First, *how does BeamAdapt perform uplink CSI estimation?* Second, *how does BeamAdapt obtain the received SINR to perform the beamforming size adaptation?* We next answer them below.

6.1.1 Uplink CSI Estimation

Due to the absence of uplink/downlink channel reciprocity in cellular network [18], we can only adopt closed-loop CSI estimation in BeamAdapt (see Section 2.2). That is, the client concatenates a short field made up of several training symbols to the data field in each uplink frame. Seeing the training symbols, the base station estimates uplink CSI and sends it back to the client. Thanks to the full-duplex property of cellular channels, the estimated CSI can be simultaneously delivered to the client through downlink control

signaling while the client is involved in uplink transmission. Therefore, CSI feedback does not incur any additional uplink channel occupation. Moreover, the training field can be very short compared to the entire frame, i.e. a 16μs training field for beamforming size of four and a 10ms frame in UMTS and LTE [18], which further render the overhead of CSI estimation negligible. According to our measurement in Chapter 3.2, the 10ms frame length in UMTS/LTE guarantees accurate CSI estimation of BeamAdapt, even with client rotation.

6.1.2 Beam Adaptation

To adapt the beamforming size and transmit power, BeamAdapt needs to know the received SINR of each frame. While it can be similarly sent back to the client through downlink control signaling, we seek to minimize the protocol modification, by leveraging the uplink power control mechanism inherent in cellular protocols. Uplink power control is widely used in cellular protocols to maintain a constant SINR of each client at the base station. It is initiated by the base station, through sending a power control command to the client, containing the value of required transmit power. Noticeably, this required transmit power is actually P_O in Equation (2), and one can directly identify the optimal transmit power P_{TX} and beamforming size N using P_O, as one iteration in the BeamAdapt algorithm. This way, the received SINR is no longer needed and no protocol changed is required.

6.2 Simulation Setup

Since the beamforming hardware is not included in Qualnet, we have to virtually realize a beamforming system on the client by generating dynamic beamforming patterns

in real-time and adopting the power model in Section 2.3 to calculate client power consumption.

We use the same network configuration shown in Figure 5 (a), and assume the UMTS protocol in Qualnet. However, here we add more clients, i.e. thirty, to mimic realistic base station scheduling and handoff in cellular networks. The area is 4km×4km and the base stations have fixed locations, 1.5km from its neighbors. While the range of each base station is approximately 1km, we let their coverage overlap similar to realistic cellular networks in urban areas. The clients are allowed to have movement with random speed from zero to seventy miles per hour, corresponding to a wide range of client movement speed such as stationary, pedestrian and vehicular. We also incorporate client rotation with an upper bounded speed of 120°/s [1]. We add two applications to the client: FTP with an unlimited-size file to transfer and constant-bit-rate (CBR) with multiple relatively small packets. FTP generates continuous traffic. CBR, on the contrary, creates intermittent traffic by the idle intervals between the small-size packets. Therefore, the FTP traffic has a higher capacity requirement than the CBR traffic.

We evaluate the power reduction benefit of BeamAdapt by comparing it with omni directional transmission and static beamforming with a fixed beamforming size. We examine BeamAdapt and static beamforming (BF) with two, four and eight antennas. Note that BeamAdapt with N=4 means that the client can select from one to four active antennas (with unused antennas powered off) while BF with N=4 always uses four active antennas.

6.3 Findings

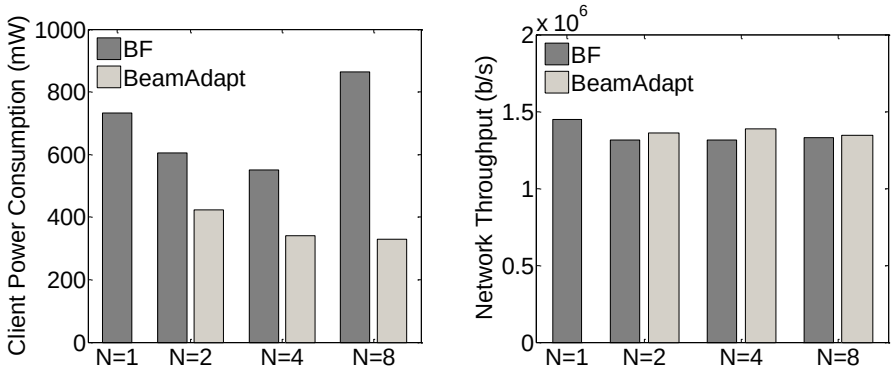

(a) FTP traffic

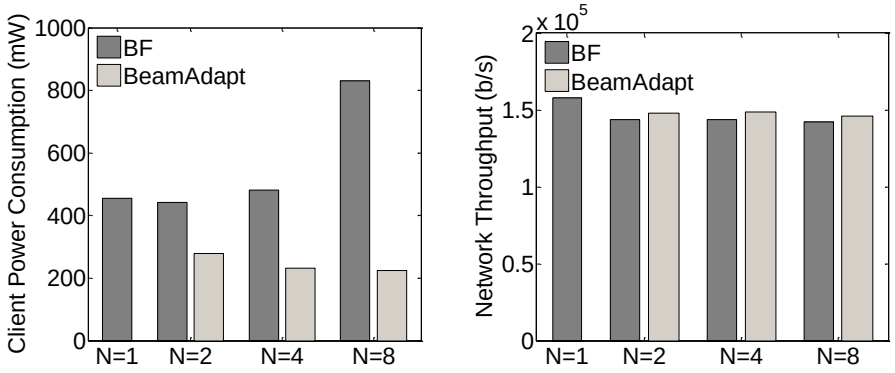

(b) CBR traffic

Figure 11: Client power consumption and network throughput comparison between BeamAdapt and static beamforming.

Figure 11 shows the average power consumption of the client as well as the network throughput, under omni, static beamforming and BeamAdapt. We make several key observations. (*i*) Firstly, since the FTP traffic averagely requires higher transmit power, BeamAdapt saves more power. For example, compared to omni directional transmission BeamAdapt with N=4 saves 54% and 50% client power for the FTP and CBR traffic, respectively. (*ii*) Secondly, BeamAdapt with four antennas already provides power efficiency benefit. The power reduction of BeamAdapt with N=8 is only marginally

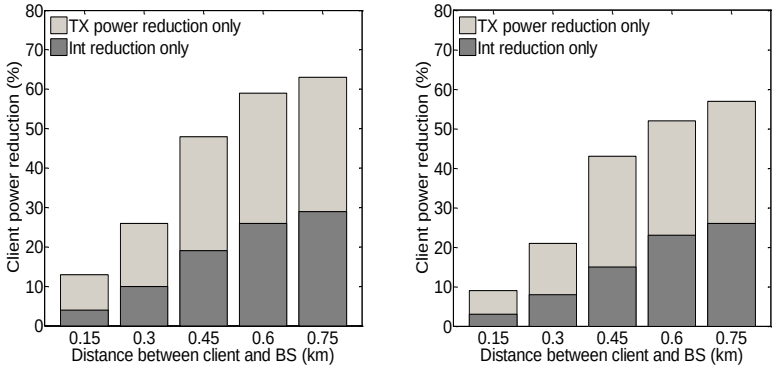

Figure 12: Breakdown of client power reduction by BeamAdapt.

better than that of BeamAdapt with N=4. This is due to the confined range of cellular radio signal and the corresponding maximal transmit power limit. (*iii*) Finally, the network throughput achieved by BeamAdapt is only slightly lower (<5%) than that by omni directional transmission, and is as good as that by their respective static beamforming counterparts. The slight degradation is due to client mobility and thereby the drop of the beamforming gain, similar to what we observed in Chapter 3.2.

We also note that the power reduction by BeamAdapt stems from two benefits of beamforming: the improvement of SNR and the reduction of interference. Qualnet simulation allows us to further examine the power saving contribution from these two benefits. That is, we first only keep the transmit power reduction capability of BeamAdapt and then the interference reduction capability only. Figure 12 shows their respective contribution to client power reduction, with different distance from the client to the base station. Clearly, as the client moves to cell boundary, i.e. with a larger distance to the base station, both capabilities can save more power, and they collectively achieve a higher overall power reduction of the client. This is because when the client is

approaching cell boundary, only not the required transmit power increases, but also the interference between adjacent cells is more severe.

Chapter 7 **Related Work**

Our work is the first that aims to enable real-time and power efficient beamforming on mobile devices. Nonetheless, multi-antenna techniques and directional communication have been generally studied in many other regimes. We next discuss related work.

7.1 Beamforming

No existing work on beamforming has considered and optimized its use on mobile devices such as Tablets and smartphones. Recent work such as [10, 11] considered using beamforming on vehicles to enhance the uplink connection as the client moves. The authors of [19] have experimentally shown the effectiveness of switched beam systems in indoor environments. However, all of above solutions use the Phocus Array system [8] and none supports real-time beamforming. More importantly, these solutions do not consider dynamic number of active antennas in beamforming and its power efficiency benefit.

7.2 Directional Antennas on Mobile Devices

Passive directional antenna is an efficient yet inflexible way to realize directional communication. Many have studied them for infrastructure nodes and mobile nodes that do not rotate, e.g. see [20-27]. Most of the authors focus on MAC protocol designs. In contrast, BeamAdapt is in the PHY layer and is complementary to directional MAC designs. Only very recently, the authors of [1, 28] demonstrated the effectiveness of passive directional antennas in improving transmission throughput and power efficiency of mobile devices that can rotate like Smartphones. The solution is based on selecting one

out of multiple fixed passive directional antennas. However, there is a key limitation toward their solution: only a limited number of passive antennas are allowed to be implemented, e.g. four in [1], and they are hard to be properly oriented. Such limitation renders a confined gain of their solution due to failure to cover all directions, i.e. only 3dB gain using 5dBi and 8dBi antennas. In contrast, beamforming with BeamAdapt can easily track channel variation and achieves a guaranteed gain of 6dB using four antennas.

7.3 Power Efficient MIMO

While in this work we consider beamforming for its adaptive use in a power efficient manner, similar concept can be extended to MIMO systems. The authors of [29] have provided a system design of an adaptive MIMO system and experimentally shown that it can minimize the energy per bit of the MIMO transceiver by properly choosing the number of active RF chains. The idea is also explored by the authors of [30] and [31]. The authors of [32] have analytically showed the effectiveness and performance of such adaptive MIMO systems. These solutions, however, are limited to a single link, while BeamAdapt is solving a network problem by optimizing the use of beamforming on multiple mobile clients.

Chapter 8 **Conclusion**

In this work, we reported a first study of beamforming on mobile devices. With both experiments and data from industry, we showed that beamforming is not only feasible but also power efficient to mobile devices. We then addressed the challenge of identifying the optimal use of beamforming on mobile device by formulating an optimization problem and providing the BeamAdapt solution. Through both experiments and simulation, we showed that BeamAdapt is able to react to client mobility by promptly identifying the right beamforming size and the transmit power. Collectively it achieves more than 50% power reduction of the clients in a large-scale network.

Client directionality through beamforming is a radical departure from omni directionality assumed by current mobile network paradigms. While we are able to demonstrate its benefit in client efficiency, more research at various layers of the network system is required to fully appreciate its potential, which we leave to future work.

REFERENCE

[1] T. Sarkar, *Smart antennas*: Wiley-Interscience Hoboken, NJ, 2003.

[2] A. J. Paulraj, D. A. Gore, R. U. Nabar, and H. Bolcskei, "An Overview of MIMO Communications—A Key to Gigabit Wireless," *Proc. IEEE,* vol. 92, pp. 198-218, 2004.

[3] H. Yu, L. Zhong, and A. Sabharwal, "Adaptive RF chain management for energy-efficient spatial-multiplexing MIMO transmission," in *Proc. ACM/IEEE Int. Symp. Low Power Electronics and Design* San Fancisco, CA, USA: ACM, 2009.

[4] L. C. Godara, *Smart Antennas*: CRC Press, 2004.

[5] M. Blanco, R. Kokku, K. Ramachandran, S. Rangarajan, and K. Sundaresan, "On the Effectiveness of Switched Beam Antennas in Indoor Environments," in *Passive and Active Network Measurement*, 2008, pp. 122-131.

[6] X. Liu, A. Sheth, M. Kaminsky, K. Papagiannaki, S. Seshan, and P. Steenkiste, "DIRC: increasing indoor wireless capacity using directional antennas," in *Proc. SIGCOMM* Barcelona, Spain: ACM, 2009.

[7] V. Navda, A. P. Subramanian, K. Dhanasekaran, A. Timm-Giel, and S. Das, "MobiSteer: using steerable beam directional antenna for vehicular network access," in *Proc. Int. Conf. Mobile Systems, Applications and Services (MobiSys)*, 2007, pp. 192-205.

[8] K. Ramachandran, R. Kokku, K. Sundaresan, M. Gruteser, and S. Rangarajan, "R2D2: regulating beam shape and rate as directionality meets diversity," in *Proc. MobiSys* Poland: ACM, 2009.

[9] D. G. Rahn, M. S. Cavin, F. F. Dai, N. H. W. Fong, R. Griffith, J. Macedo, A. D. Moore, J. W. M. Rogers, and M. Toner, "A fully integrated multiband MIMO WLAN transceiver RFIC," *IEEE Journal of Solid-State Circuits,* vol. 40, pp. 1629-1641, 2005.

[10] S. Cui, A. J. Goldsmith, and A. Bahai, "Energy-efficiency of MIMO and cooperative MIMO techniques in sensor networks," *IEEE Journal on Selected Areas in Communications,* vol. 22, pp. 1089-1098, 2004.

[11] Z. Li, W. Ni, J. Ma, M. Li, D. Ma, D. Zhao, J. Mehta, D. Hartman, X. Wang, K. K. O, and K. Chen, "A Dual-Band CMOS Transceiver for 3G TD-SCDMA," in *Solid-State Circuits Conference, 2007. ISSCC 2007. Digest of Technical Papers. IEEE International*, 2007, pp. 344-607.

[12] Z. Xu, S. Jiang, Y. Wu, H.-y. Jian, G. Chu, K. Ku, P. Wang, N. Tran, Q. Gu, M.-z. Lai, C. Chien, M. F. Chang, and R. D. Chow, "A compact dual-band direct-conversion CMOS transceiver for 802.11a/b/g WLAN," in *IEEE Int. Solid-State Circuits Conf. (ISSCC)*, 2005, pp. 98-586 Vol. 1.

[13] IEEE International Solid State Circuits Conference, *http://www.isscc.org*.

[14] IEEE Journal of Solid-State Circuits.

[15] K. Vavelidis, I. Vassiliou, T. Georgantas, A. Yamanaka, S. Kavadias, G. Kamoulakos, C. Kapnistis, Y. Kokolakis, A. Kyranas, P. Merakos, I. Bouras, S. Bouras, S. Plevridis, and N. Haralabidis, "A dual-band 5.15-5.35-GHz, 2.4-2.5-GHz 0.18um CMOS transceiver for 802.11a/b/g wireless LAN," *IEEE Journal of Solid-State Circuits,* vol. 39, pp. 1180-1184, 2004.

[16] A. Pozsgay, T. Zounes, R. Hossain, M. Boulemnakher, V. Knopik, and S. Grange, "A Fully Digital 65nm CMOS Transmitter for the 2.4-to-2.7GHz WiFi/WiMAX Bands using 5.4GHz RF DACs," in *IEEE Int. Solid-State Circuits Conf. (ISSCC)*, 2008, pp. 360-619.

[17] WARP, *http://warp.rice.edu/*, 2010.

[18] C.-K. Chau, M. Chen, and S. C. Liew, "Capacity of large-scale CSMA wireless networks," in *Proc. MobiCom* Beijing, China: ACM, 2009.

[19] G. L. Nemhauser and L. A. Wolsey, *Integer and combinatorial optimization*: Wiley-Interscience, 1988.

[20] G. J. Foschini and Z. Miljanic, "A simple distributed autonomous power control algorithm and its convergence," *IEEE Transactions on Vehicular Technology*, vol. 42, pp. 641-646, 1993.

[21] E. Dahlman, S. Parkvall, J. Skold, and P. Beming, *3G Evolution, Second Edition: HSPA and LTE for Mobile Broadband*: Academic Press, 2008.

[22] Scalable Network Technologies, *QualNet Developer: High-fidelity network evaluation software*.

[23] F. Rashid-Farrokhi, L. Tassiulas, and K. J. R. Liu, "Joint optimal power control and beamforming in wireless networks using antenna arrays," *IEEE Trans. Communications*, vol. 46, pp. 1313-1324, 1998.

[24] R. Knopp and G. Caire, "Power control and beamforming for systems with multiple transmit and receive antennas," *IEEE Trans. Wireless Communications*, vol. 1, p. 638, 2002.

[25] S. Yi, Y. Pei, and S. Kalyanaraman, "On the capacity improvement of ad hoc wireless networks using directional antennas," in *Proc. MobiHoc* Annapolis, Maryland, USA: ACM, 2003.

[26] L. Bao and J. J. Garcia-Luna-Aceves, "Transmission scheduling in ad hoc networks with directional antennas," in *Proc. MobiCom* Atlanta, Georgia, USA: ACM, 2002.

[27] K. Young-Bae, V. Shankarkumar, and N. H. Vaidya, "Medium access control protocols using directional antennas in ad hoc networks," in *INFOCOM*, 2000, pp. 13-21 vol.1.

[28] T. Korakis, G. Jakllari, and L. Tassiulas, "A MAC protocol for full exploitation of directional antennas in ad-hoc wireless networks," in *Proc. ACM Int. Sym. Mobile Ad Hoc Networking & Computing (MobiHoc)* Annapolis, Maryland, USA, 2003, pp. 98-107.

[29] R. R. Choudhury, X. Yang, R. Ramanathan, and N. H. Vaidya, "Using directional antennas for medium access control in ad hoc networks," in *Proc. ACM Int. Conf. Mobile Computing and Networking (MobiCOM)* Atlanta, GA, 2002.

[30] M. Takai, J. Martin, R. Bagrodia, and A. Ren, "Directional virtual carrier sensing for directional antennas in mobile ad hoc networks," in *Proc. MobiHoc* Lausanne, Switzerland: ACM, 2002.

[31] A. Amiri Sani, H. Dumanli, L. Zhong, and A. Sabharwal, "Power-efficient directional wireless communication on small form-factor mobile devices," in *Proc. ISLPED*: ACM/IEEE, 2010.

[32] A. Amiri Sani, L. Zhong, and A. Sabharwal, "Directional antenna diversity for mobile devices: characterizations and solutions," in *Proc. MobiCom*: ACM, 2010.

[33] S. Venkatesan, A. Lozano, and R. Valenzuela, "Network MIMO: Overcoming intercell interference in indoor wireless systems," in *Proc. Asilomar*, 2007, pp. 83–87.